Energy-momentum time integrations of a non-isothermal two-phase dissipation model for fiber-reinforced materials based on a virtual power principle

Michael Groß, Julian Dietzsch, Chris Röbiger

Energy-momentum time integrations of a non-isothermal two-phase dissipation model for fiber-reinforced materials based on a virtual power principle

Michael Groß, Julian Dietzsch, Chris Röbiger

Professorship of Applied Mechanics and Dynamics
Faculty of Mechanical Engineering

ECCOMAS Coupled 2019 June 4, 2019

MS: Thermo Mechanical Problems III

Acknowledgment: This research is provided by DFG under the grant GR 3297

TECHNISCHE UNIVERSITÄT CHEMNITZ

Motivation: Dynamical FE simulations of hybrid woven composites

Combination of natural and inorganic fabrics: Improved vibration damping

1. Natural fiber: flax, hemp, jute
2. Inorganic fiber: carbon, glass, aramid

Michael Carus [2015] (nova-Institut GmbH)

Gareth Davies [2018] (Composites Evolution)

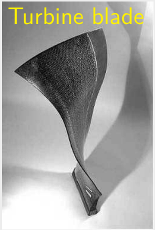

De Luycker, Morestin, Boisse, Marsal [2009]

Mesoscopic scale: Volume element (RVE)

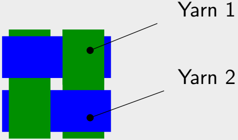

Microscopic scale: Yarn with bending stiffness

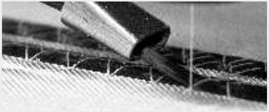

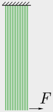

Kai Uhlig [2017] (IPF TU Dresden), recommended by IST TU Chemnitz

Goals: Variational formulations which take into account secondary effects

1. Design of energy-momentum schemes for stable dynamical FE simulations

Strategy (I): Matrix and fiber viscoelasticity

(see e.g. Nedjar [2007])

Modelling of anisotropic Cauchy continua with structural tensors

(see e.g. Reese et al. [2001], Klinkel et al. [2005], Schröder et al. [2005])

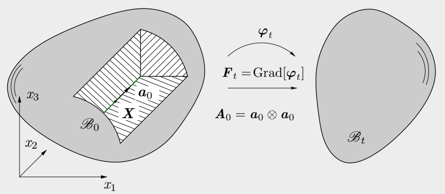

Matrix material with isotropic viscoelasticity

(see e.g. Govindjee & Reese [1997])

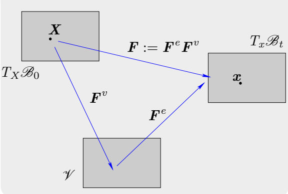

Fiber viscoelasticity with linear space $\mathscr{V}_F$ ('intermediate configuration')

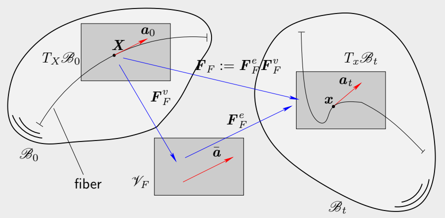

Numerical integration of the viscous evolution

1. **Matrix material model:** solved pointwise (ODE) at spatial quadrature points
2. **Fiber material model:** solved elementwise with spatial element nodes

Strategy (II): Generalized continuum mechanics

(see e.g. Boisse et al. [2018], Asmanoglo & Menzel [2017], Madeo et al. [2015], Feretti et al. [2014], Spencer & Soldatos [2007])

Three point bending test: experiment vs. Cauchy theory $\rightsquigarrow$ 'the need to a second-gradient theory' (see Madeo et al. [2015], Charmetant et al. [2012])

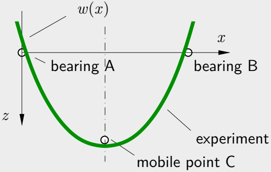

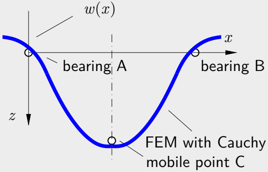

Introduction of skew-symmetric stress/drilling degrees of freedom

(see e.g. Hughes & Brezzi [1989], Ibrahimbegovic et al. [1990,1991,1993], Choi et al. [2002], Boujelben & Ibrahimbegovic [2017])

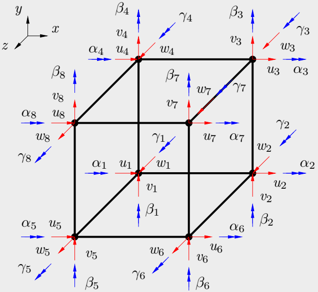

Timoshenko beam (with secondary effects)

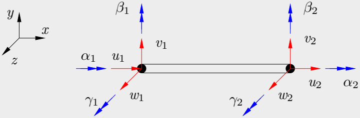

1. **Does not overestimate bending stiffness**
2. **Does not overestimate natural frequencies**

Cauchy continuum model (I)

Transversely isotropic (first-order gradient) material

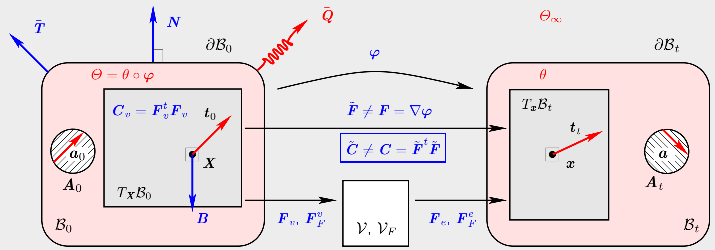

Deformation of fibers and matrix (cf. Klinkel et al. [2005], Nedjar [2007])

1. Deformation of the fibers

$$F_F := a_t \otimes a_0 = \tilde{F} A_0 \qquad A_0 := a_0 \otimes a_0 \qquad C_F := F_F^t F_F := C_F A_0$$

2. Fiber and volume dilatation

$$\tilde{C}_F \neq C_F := \tilde{C} : A_0 \qquad \tilde{C}_V \neq C_V := [\det(\tilde{C})]^{\frac{1}{n_{\dim}}}$$

3. Viscoelastic matrix and fibers

$$F = F_e F_v \qquad C_v = F_v^t F_v \qquad F_F = F_F^e F_F^v \qquad C_F^v = \tilde{C}_F^v A_0$$

Cauchy continuum model (II)

Viscous evolution equations (cf. Reese [2001], Nedjar [2007], Krüger et. al. [2011])

1. Viscous matrix evolution equation and non-equilibrium stress tensor

$$\boxed{\boldsymbol{Y} = \boldsymbol{\Sigma}_v} \qquad \boldsymbol{Y} := -\frac{\partial \Psi_M^{\text{vis}}}{\partial \boldsymbol{C}_v} \qquad D_M^{\text{int}} := \dot{\boldsymbol{C}}_v : \boldsymbol{\Sigma}_v = \dot{\boldsymbol{C}}_v : \mathbb{V}(\boldsymbol{C}_v) : \dot{\boldsymbol{C}}_v \geq 0$$

$$\mathbb{V}(\boldsymbol{C}_v) = \frac{1}{4}\left[V_{\text{vol}} - \frac{V_{\text{dev}}}{n_{\text{dim}}}\right] \boldsymbol{C}_v^{-1} \otimes \boldsymbol{C}_v^{-1} + \frac{V_{\text{dev}}}{4}\,\mathbb{I}^{\text{sym}} : \boldsymbol{C}_v^{-1} \otimes \boldsymbol{C}_v^{-1}$$

2. Viscous fiber evolution equation and non-equilibrium stress

$$\boxed{Y_F = \Sigma_F^v} \qquad Y_F := -\frac{\partial \Psi_F^{\text{vis}}}{\partial C_F^v} \qquad D_F^{\text{int}} := \dot{C}_F^v\, \Sigma_F^v = \dot{C}_F^v \, \frac{V_F}{4\,(C_F^v)^2}\, \dot{C}_F^v \geq 0$$

Thermo-viscoelastic free energy

1. Hyperelastic strain energy

$$\Psi^{\text{ela}}(\tilde{\boldsymbol{C}}, \tilde{C}_V, \tilde{C}_F; \boldsymbol{A}_0) = \hat{\Psi}_M^{\text{iso}}(I_1^{\tilde{C}}, I_2^{\tilde{C}}, I_3^{\tilde{C}}, I_4) + \hat{\Psi}_M^{\text{vol}}(\tilde{C}_V) + \hat{\Psi}_F^{\text{ela}}(\tilde{C}_F)$$

2. Thermoelastic free energy

$$\begin{aligned}\Psi^{\text{the}}(\Theta, \tilde{C}_V, \tilde{C}_F) = \; & \hat{\Psi}^{\text{cap}}(\Theta) - 2\sqrt{\tilde{C}_V{}^{2-n_{\text{dim}}}}\; \beta_M\,[\Theta - \Theta_\infty]\, \mathrm{D}\hat{\Psi}_M^{\text{vol}}(\tilde{C}_V) \\ & - 2\sqrt{\tilde{C}_F^{2-1}}\; \beta_F\,[\Theta - \Theta_\infty]\, \mathrm{D}\hat{\Psi}_F^{\text{ela}}(\tilde{C}_F)\end{aligned}$$

3. Viscoelastic free energy

$$\Psi_M^{\text{vis}}(\tilde{\boldsymbol{C}}, \boldsymbol{C}_v) = \hat{\Psi}_M^{\text{ela}}(I_1^{\tilde{C}C_v^{-1}}, I_2^{\tilde{C}C_v^{-1}}, I_3^{\tilde{C}C_v^{-1}}) \qquad \Psi_F^{\text{vis}}(\tilde{C}_F, \tilde{C}_F^v) = \Psi_F^{\text{ela}}(\tilde{C}_F[\tilde{C}_F^v]^{-1})$$

Generalized Cauchy virtual power principle (I)

Total energy balance law in functional form

$$\dot{\mathcal{H}}(\underbrace{\boldsymbol{\varphi}, \dot{\boldsymbol{v}}, \dot{\boldsymbol{p}}, \dot{\boldsymbol{\alpha}}, \dot{\boldsymbol{\omega}}, \dot{\boldsymbol{\pi}}, \dot{\boldsymbol{C}}_v, \dot{\Theta}, \dot{\eta}, \dot{\tilde{\boldsymbol{F}}}, \dot{\tilde{\boldsymbol{C}}}, \dot{\tilde{C}}_V, \dot{\tilde{C}}_F, \dot{\tilde{C}}_F^v}_{\text{temporally continuous}}, \underbrace{\tilde{\Theta}, \boldsymbol{P}, \boldsymbol{\tau}^t_{\text{skw}}, \boldsymbol{S}, S_V, S_F, \boldsymbol{R}, h, \lambda, \boldsymbol{Z}, \hat{\boldsymbol{\omega}}}_{\text{temporally discontinuous}}) = 0 \qquad \dot{\mathcal{H}} = \dot{\mathcal{T}}^{\text{tra}} + \dot{\mathcal{T}}^{\text{rot}} + \dot{\Pi}^{\text{ext}} + \dot{\Pi}^{\text{int}}$$

Kinetic power functionals

(motivated by Altenbach et al. [2003], Askes & Aifantis [2011])

$$\dot{\mathcal{T}}^{\text{tra}}(\dot{\boldsymbol{\varphi}}, \dot{\boldsymbol{v}}, \dot{\boldsymbol{p}}) := \int_{\mathscr{B}_0} [\rho_0 \boldsymbol{I}\, \boldsymbol{v} - \boldsymbol{p}] \cdot \dot{\boldsymbol{v}} \,\mathrm{d}V - \int_{\mathscr{B}_0} \dot{\boldsymbol{p}} \cdot [\boldsymbol{v} - \dot{\boldsymbol{\varphi}}] \mathrm{d}V + \int_{\mathscr{B}_0} \boldsymbol{p} \cdot \ddot{\boldsymbol{\varphi}} \,\mathrm{d}V$$

$$\dot{\mathcal{T}}^{\text{rot}}(\dot{\boldsymbol{\alpha}}, \dot{\boldsymbol{\omega}}, \dot{\boldsymbol{\pi}}) := \int_{\mathscr{B}_0} \left[\rho_0 \left[(l_F^2 - l_0^2)\, \boldsymbol{A}_0 + l_0^2 \boldsymbol{I}\right] \boldsymbol{\omega} - \boldsymbol{\pi}\right] \cdot \dot{\boldsymbol{\omega}} \,\mathrm{d}V - \int_{\mathscr{B}_0} \dot{\boldsymbol{\pi}} \cdot [\boldsymbol{\omega} - \dot{\boldsymbol{\alpha}}] \mathrm{d}V + \int_{\mathscr{B}_0} \boldsymbol{\pi} \cdot \ddot{\boldsymbol{\alpha}} \,\mathrm{d}V$$

External power functional

$$D^{\text{cdu}} = -\nabla(\ln \Theta) \cdot \boldsymbol{Q}$$

$$\begin{aligned}
\dot{\Pi}^{\text{ext}} := &- \int_{\mathscr{B}_0} \rho_0 \boldsymbol{B} \cdot \dot{\boldsymbol{\varphi}} \,\mathrm{d}V - \int_{\partial_T \mathscr{B}_0} \bar{\boldsymbol{T}} \cdot \dot{\boldsymbol{\varphi}} \,\mathrm{d}A + \int_{\partial_Q \mathscr{B}_0} \frac{\tilde{\Theta}}{\Theta} \bar{Q} \,\mathrm{d}A \\
&+ \int_{\mathscr{B}_0} \frac{1}{\Theta} \nabla \tilde{\Theta} \cdot \boldsymbol{Q} \,\mathrm{d}V + \int_{\mathscr{B}_0} \frac{\tilde{\Theta}}{\Theta} \left(D^{\text{cdu}} + D^{\text{int}}\right) \mathrm{d}V + \int_{\mathscr{B}_0} \dot{\boldsymbol{C}}_v : \boldsymbol{\Sigma}_v \,\mathrm{d}V \\
&+ \int_{\partial_\Theta \mathscr{B}_0} \lambda \left[\tilde{\Theta} - \Theta_\infty\right] \mathrm{d}A - \int_{\partial_{\dot{\Theta}} \mathscr{B}_0} h \left[\dot{\Theta} - \dot{\bar{\Theta}}\right] \mathrm{d}A - \int_{\partial_\varphi \mathscr{B}_0} \boldsymbol{R} \cdot \left[\dot{\boldsymbol{\varphi}} - \dot{\bar{\boldsymbol{\varphi}}}\right] \mathrm{d}A \\
&- \int_{\partial_\alpha \mathscr{B}_0} \boldsymbol{Z} \cdot \left[\dot{\boldsymbol{\alpha}} - \dot{\bar{\boldsymbol{\alpha}}}\right] \mathrm{d}A - \int_{\partial_\alpha \mathscr{B}_0} \hat{\boldsymbol{\omega}} \cdot \left[\boldsymbol{\epsilon} : \boldsymbol{\tau}^t_{\text{skw}}\right] \mathrm{d}A - \int_{\partial_W \mathscr{B}_0} \bar{\boldsymbol{W}} \cdot \dot{\boldsymbol{\alpha}} \,\mathrm{d}A \\
&+ \int_{\mathscr{B}_0} \frac{1}{2} \bar{\boldsymbol{S}} : \dot{\tilde{\boldsymbol{C}}} \,\mathrm{d}V + \int_{\mathscr{B}_0} \frac{1}{2} \bar{S}_V\, \dot{\tilde{C}}_V \,\mathrm{d}V + \int_{\mathscr{B}_0} \frac{1}{2} \bar{S}_F\, \dot{\tilde{C}}_F \,\mathrm{d}V \\
&+ \int_{\mathscr{B}_0} \dot{\tilde{C}}_F^v\, \Sigma_F^v \,\mathrm{d}V + \int_{\mathscr{B}_0} \bar{M}_F^v \left[L_F(\dot{\tilde{C}}_F) - L_F(\dot{\tilde{C}}_F^v)\right] \mathrm{d}V \quad \text{with} \quad L_F(\dot{\epsilon}) = \frac{\dot{\overline{\ln(\epsilon)}}}{2}
\end{aligned}$$

Generalized Cauchy virtual power principle (II)

Internal power functional

(motivated by Steinmann & Stein [1997])

$$\begin{aligned}
\dot{\Pi}^{\mathrm{int}} := \; & \frac{1}{2}\int_{\mathscr{B}_0}\left\{\left[2\,\frac{\partial\hat{\Psi}_M}{\partial\tilde{\boldsymbol{C}}} + S_V\,\boldsymbol{A}^{\mathrm{vol}} + S_F\,\boldsymbol{A}_0 - \boldsymbol{S}\right]:\dot{\tilde{\boldsymbol{C}}} + \left[2\,\frac{\partial\hat{\Psi}_M}{\partial\tilde{C}_V} - S_V\right]:\dot{\tilde{C}}_V\right\}\mathrm{d}V - \int_{\mathscr{B}_0}\dot{\eta}\,[\tilde{\Theta}-\Theta]\,\mathrm{d}V \\
& + \frac{1}{2}\int_{\mathscr{B}_0}\left[2\,\frac{\partial\hat{\Psi}_F}{\partial\tilde{C}_F} - S_F\right]:\dot{\tilde{C}}_F\,\mathrm{d}V + \int_{\mathscr{B}_0}\left\{\left[\tilde{\boldsymbol{F}}\boldsymbol{S} - \boldsymbol{P}\right]:\dot{\tilde{\boldsymbol{F}}} + \frac{\partial\hat{\Psi}_M}{\partial\boldsymbol{C}_v}:\dot{\boldsymbol{C}}_v\right\}\mathrm{d}V + \int_{\mathscr{B}_0}\left[\eta + \frac{\partial\Psi}{\partial\Theta}\right]\dot{\Theta}\,\mathrm{d}V \\
& + \int_{\mathscr{B}_0}\boldsymbol{P}:\nabla\dot{\boldsymbol{\varphi}}\,\mathrm{d}V + \int_{\mathscr{B}_0}\boldsymbol{\tau}^t_{\mathrm{skw}}:\left[\mathbb{I}^{\mathrm{skw}}:\dot{\tilde{\boldsymbol{F}}}\tilde{\boldsymbol{F}}^{-1} + \boldsymbol{\epsilon}\cdot\dot{\boldsymbol{\alpha}}\right]\mathrm{d}V + \int_{\mathscr{B}_0}\frac{\partial\Psi_F}{\partial\tilde{C}^v_F}\,\dot{\tilde{C}}^v_F\,\mathrm{d}V \quad \text{with} \quad 2\,\mathbb{I}^{\mathrm{skw}} = \boldsymbol{\epsilon}\cdot\boldsymbol{\epsilon}
\end{aligned}$$

Principle of virtual power

$$\delta_*\dot{\mathcal{H}}(\underbrace{\dot{\boldsymbol{\varphi}},\dot{\boldsymbol{v}},\dot{\boldsymbol{p}},\dot{\boldsymbol{\alpha}},\dot{\boldsymbol{\omega}},\dot{\boldsymbol{\pi}},\dot{\boldsymbol{C}}_v,\dot{\Theta},\dot{\eta},\dot{\tilde{\boldsymbol{F}}},\dot{\tilde{\boldsymbol{C}}},\dot{\tilde{C}}_V,\dot{\tilde{C}}_F,\dot{\tilde{C}}^v_F}_{\text{temporally continuous}},\underbrace{\tilde{\Theta},\boldsymbol{P},\boldsymbol{\tau}^t_{\mathbf{skw}},\boldsymbol{S},S_V,S_F,\boldsymbol{R},h,\lambda,\boldsymbol{Z},\hat{\boldsymbol{\omega}}}_{\text{temporally discontinuous}}) = 0$$

Non-standard weak forms (compared to the Cauchy continuum)

$$\int_{\mathscr{B}_0}\delta_*\boldsymbol{\tau}^t_{\mathrm{skw}}:\boldsymbol{\epsilon}\cdot\left[\frac{1}{2}\boldsymbol{\epsilon}:\dot{\tilde{\boldsymbol{F}}}\tilde{\boldsymbol{F}}^{-1} + \dot{\boldsymbol{\alpha}}\right]\mathrm{d}V = \int_{\partial_\alpha\mathscr{B}_0}\hat{\boldsymbol{\omega}}\cdot\boldsymbol{\epsilon}:\delta_*\boldsymbol{\tau}^t_{\mathrm{skw}}\,\mathrm{d}A \qquad \int_{\partial_\alpha\mathscr{B}_0}\delta_*\hat{\boldsymbol{\omega}}\cdot\boldsymbol{\epsilon}:\boldsymbol{\tau}^t_{\mathrm{skw}}\,\mathrm{d}A = \boldsymbol{0}$$

$$\int_{\mathscr{B}_0}\delta_*\dot{\boldsymbol{\alpha}}\cdot\left[\dot{\boldsymbol{\pi}} + \boldsymbol{\epsilon}:\boldsymbol{\tau}^t_{\mathrm{skw}}\right]\mathrm{d}V = \int_{\partial_\alpha\mathscr{B}_0}\delta_*\dot{\boldsymbol{\alpha}}\cdot\boldsymbol{Z}\,\mathrm{d}A + \int_{\partial_W\mathscr{B}_0}\delta_*\dot{\boldsymbol{\alpha}}\cdot\bar{\boldsymbol{W}}\,\mathrm{d}A \qquad \int_{\partial_\alpha\mathscr{B}_0}\delta_*\boldsymbol{Z}:\left[\dot{\boldsymbol{\alpha}} - \dot{\bar{\boldsymbol{\alpha}}}\right]\mathrm{d}V = \boldsymbol{0}$$

$$\int_{\mathscr{B}_0}\delta_*\dot{\boldsymbol{\omega}}\cdot\left[\rho_0\left[(l_F^2 - l_0^2)\,\boldsymbol{A}_0 + l_0^2\boldsymbol{I}\right]\boldsymbol{\omega} - \boldsymbol{\pi}\right]\mathrm{d}V = \boldsymbol{0} \qquad \int_{\mathscr{B}_0}\delta_*\dot{\boldsymbol{\omega}}\cdot\left[\boldsymbol{\omega} - \dot{\boldsymbol{\alpha}}\right]\mathrm{d}V = \boldsymbol{0}$$

$$\int_{\mathscr{B}_0}\delta_*\dot{\tilde{\boldsymbol{F}}}:\left[\tilde{\boldsymbol{F}}\tilde{\boldsymbol{S}} + \boldsymbol{\tau}^t_{\mathrm{skw}}\tilde{\boldsymbol{F}}^{-t} - \boldsymbol{P}\right]\mathrm{d}V = \boldsymbol{0} \qquad \int_{\mathscr{B}_0}\delta_*\boldsymbol{P}:\left[\dot{\tilde{\boldsymbol{F}}} - \mathrm{Grad}\,[\dot{\boldsymbol{\varphi}}]\right]\mathrm{d}V = \boldsymbol{0}$$

Additional balance laws

Balance law of angular momentum $\mathcal{J}$ includes additively:

Balance law of rotational momentum $\mathcal{J}^{\text{rot}}$

Set $\delta_* \dot{\boldsymbol{\alpha}} = \boldsymbol{c} = $ const.:

$$\int_{t_n}^{t_{n+1}} \int_{\mathscr{B}_0} \boldsymbol{c} \cdot \left[\dot{\boldsymbol{\pi}} + \boldsymbol{\epsilon} : \boldsymbol{\tau}^t_{\text{skw}} \right] \mathrm{d}V \, \mathrm{d}t = \int_{t_n}^{t_{n+1}} \int_{\partial_\alpha \mathscr{B}_0} \boldsymbol{c} \cdot \boldsymbol{Z} \, \mathrm{d}A \, \mathrm{d}t + \int_{t_n}^{t_{n+1}} \int_{\partial_W \mathscr{B}_0} \boldsymbol{c} \cdot \bar{\boldsymbol{W}} \, \mathrm{d}A \, \mathrm{d}t$$

$$\boxed{\int_{\mathscr{B}_0} \boldsymbol{\pi}_{t_{n+1}} \, \mathrm{d}V - \int_{\mathscr{B}_0} \boldsymbol{\pi}_{t_n} \, \mathrm{d}V = (t_{n+1} - t_n) \int_{t_n}^{t_{n+1}} \left[- \int_{\mathscr{B}_0} \boldsymbol{\epsilon} : \boldsymbol{\tau}^t_{\text{skw}} \, \mathrm{d}V + \int_{\partial_\alpha \mathscr{B}_0} \boldsymbol{Z} \, \mathrm{d}A + \int_{\partial_W \mathscr{B}_0} \bar{\boldsymbol{W}} \, \mathrm{d}A \right] \mathrm{d}t}$$

Balance law of total energy $\mathcal{H}$ includes additively:

Balance law of rotational energy $\mathcal{T}^{\text{rot}}$

Set $\delta_* \dot{\boldsymbol{\alpha}} = \dot{\boldsymbol{\alpha}}$ and $\delta_* \dot{\boldsymbol{\omega}} = \dot{\boldsymbol{\omega}}$ and $\delta_* \boldsymbol{\tau}^t_{\text{skw}} = \boldsymbol{\tau}^t_{\text{skw}}$

Eqn. (1): $$\int_{t_n}^{t_{n+1}} \int_{\mathscr{B}_0} \dot{\boldsymbol{\alpha}} \cdot \left[\dot{\boldsymbol{\pi}} + \boldsymbol{\epsilon} : \boldsymbol{\tau}^t_{\text{skw}} \right] \mathrm{d}V \, \mathrm{d}t = \int_{t_n}^{t_{n+1}} \int_{\partial_\alpha \mathscr{B}_0} \dot{\boldsymbol{\alpha}} \cdot \boldsymbol{Z} \, \mathrm{d}A \, \mathrm{d}t + \int_{t_n}^{t_{n+1}} \int_{\partial_W \mathscr{B}_0} \dot{\boldsymbol{\alpha}} \cdot \bar{\boldsymbol{W}} \, \mathrm{d}A \, \mathrm{d}t$$

Eqn. (2): $$\int_{t_n}^{t_{n+1}} \int_{\mathscr{B}_0} \boldsymbol{\tau}^t_{\text{skw}} : \left[\mathbb{I}^{\text{skw}} : \dot{\tilde{\boldsymbol{F}}} \tilde{\boldsymbol{F}}^{-1} + \boldsymbol{\epsilon} \cdot \dot{\boldsymbol{\alpha}} \right] \mathrm{d}V \, \mathrm{d}t = \int_{t_n}^{t_{n+1}} \int_{\partial_\alpha \mathscr{B}_0} \hat{\boldsymbol{\omega}} \cdot \underbrace{\boldsymbol{\epsilon} : \boldsymbol{\tau}^t_{\text{skw}}}_{\boldsymbol{0}} \, \mathrm{d}A \, \mathrm{d}t$$

Eqn. (3): $$\int_{t_n}^{t_{n+1}} \int_{\mathscr{B}_0} \dot{\boldsymbol{\omega}} \cdot \left[\boldsymbol{J} \boldsymbol{\omega} - \boldsymbol{\pi} \right] \mathrm{d}V \, \mathrm{d}t = \boldsymbol{0} \qquad \text{with} \qquad \boldsymbol{J} = \rho_0 \left[(l_F^2 - l_0^2) \, \boldsymbol{A}_0 + l_0^2 \boldsymbol{I} \right]$$

$$\boxed{\begin{aligned} \mathcal{T}^{\text{rot}}_{n+1} - \mathcal{T}^{\text{rot}}_{n} \equiv{} & \frac{1}{2} \int_{\mathscr{B}_0} \boldsymbol{\omega}_{t_{n+1}} \cdot \boldsymbol{J} \boldsymbol{\omega}_{t_{n+1}} \mathrm{d}V - \frac{1}{2} \int_{\mathscr{B}_0} \boldsymbol{\omega}_{t_n} \cdot \boldsymbol{J} \boldsymbol{\omega}_{t_n} \mathrm{d}V \\ ={} & (t_{n+1} - t_n) \int_{t_n}^{t_{n+1}} \left[\int_{\mathscr{B}_0} \boldsymbol{\tau}^t_{\text{skw}} : \dot{\tilde{\boldsymbol{F}}} \tilde{\boldsymbol{F}}^{-1} \mathrm{d}V + \int_{\partial_\alpha \mathscr{B}_0} \dot{\boldsymbol{\alpha}} \cdot \boldsymbol{Z} \, \mathrm{d}A + \int_{\partial_W \mathscr{B}_0} \dot{\boldsymbol{\alpha}} \cdot \bar{\boldsymbol{W}} \, \mathrm{d}A \right] \mathrm{d}t \end{aligned}}$$

Discrete viscous fiber evolution equation

Incremental principle of virtual power

$$\int_{t_n}^{t_{n+1}} \delta_* \dot{\mathcal{H}}\, \mathrm{d}t \equiv \int_{t_n}^{t_{n+1}} \left[\delta_* \dot{\mathcal{T}} + \delta_* \dot{\varPi}^{\mathrm{int}} + \delta_* \dot{\varPi}^{\mathrm{ext}}\right] \mathrm{d}t = 0$$

Fully weak viscous fiber evolution equation

$$\int_{t_n}^{t_{n+1}} \int_{\mathscr{B}_0} \delta_* \dot{\tilde{C}}_F^v \left[-Y_F - \frac{\bar{M}_F^v}{2\,\tilde{C}_F^v} + \frac{V_F}{2\,\tilde{C}_F^v}\, L_F(\dot{\tilde{C}}_F^v) \right] \mathrm{d}V\, \mathrm{d}t = 0$$

Discrete weak form on the reference element

$$\int_0^1 \int_{\mathscr{B}_\square} \delta_* \overset{\circ}{\overline{\tilde{C}_F^v}} \left[-Y_F - \frac{\bar{M}_F^v}{2\,\tilde{C}_F^v} + \frac{V_F}{2\,\tilde{C}_F^v}\, L_F(\dot{\tilde{C}}_F^v) \right] \mathrm{d}V_\square\, \mathrm{d}\alpha = 0$$

Galerkin approximations in space and time

$$\delta_* \overset{\circ}{\overline{\tilde{C}_F^v}}(\boldsymbol{\chi}, \alpha) = \sum_{J=1}^{k} \sum_{B=1}^{\tilde{n}_{\mathrm{node}}} \tilde{M}^J(\alpha) \tilde{N}_B(\boldsymbol{\chi})\, [\tilde{C}_F^v]_J^B \qquad \tilde{C}_F^v(\boldsymbol{\chi}, \alpha) = \sum_{I=1}^{k+1} \sum_{A=1}^{\tilde{n}_{\mathrm{node}}} M^I(\alpha) \tilde{N}_A(\boldsymbol{\chi})\, [C_F^v]_I^A$$

Algorithmic fiber stress $\rightsquigarrow$ viscous evolution/equations of motion

$$\bar{M}_F^v := \mu_F^v \left[L_F(\dot{\tilde{C}}_F) - L_F(\dot{\tilde{C}}_F^v) \right] \qquad \mu_F^v := \frac{\Psi^{\mathrm{vis}}_{F_{t_{n+1}}} - \Psi^{\mathrm{vis}}_{F_{t_n}} - \int_0^1 2\, Y_F\, \tilde{C}_F^v \left[L_F(\dot{\tilde{C}}_F) - L_F(\dot{\tilde{C}}_F^v) \right] \mathrm{d}\alpha}{\int_0^1 \left[L_F(\dot{\tilde{C}}_F) - L_F(\dot{\tilde{C}}_F^v) \right]^2 \mathrm{d}\alpha}$$

Dynamic bending/torsion of a long curved pipe

(Initial-boundary conditions; 121-em with H8-mixed-Bbar-drill)

Material Status Monitor

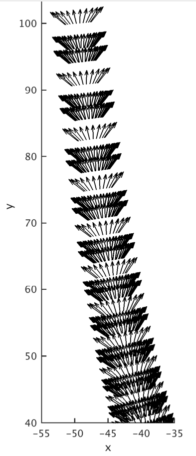

Boundary Status Monitor

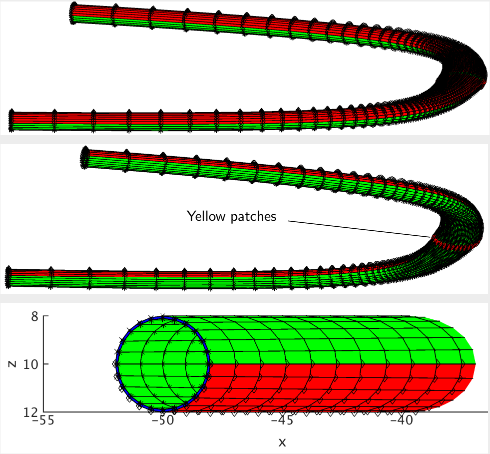

Dirichlet and Neumann boundary conditions

Yellow patches: Temperat. $\Theta^A = \Theta_\infty$, Displacem. z-dofs fixed (bearing)
Blue patches : Temperat. $\Theta^A = \Theta_\infty$, Torque load $W_x^A = \pm \hat{W}_x f(t)$
Green/red patches: no b.c. (thermal insulation $\bar{Q}^A := 0$)

Initial conditions

$\boldsymbol{\varphi}_0^A = \boldsymbol{X}^A \quad \boldsymbol{\alpha}_0^A = \mathbf{0} \quad \Theta_0^A = \Theta_\infty$

$\boldsymbol{v}_0^A = \mathbf{0} \quad \boldsymbol{\omega}_0^A = \mathbf{0} \quad \Theta_\infty = 298.15$

Dynamic bending/torsion of a long curved pipe (Motion and loads/reactions; 121-em with H8-mixed-Bbar-drill)

Current configuration with norm of rotation vector at $t_n = 0.5\,\mathrm{s}$

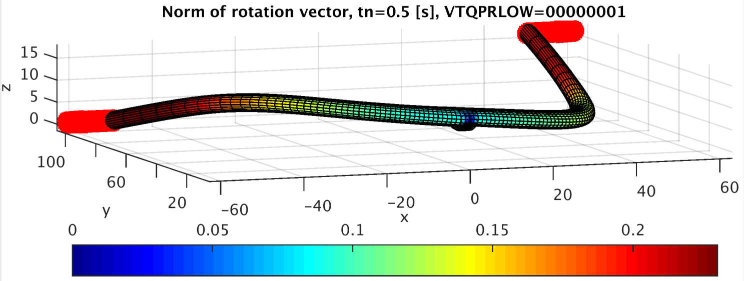

Time evolution of the loads

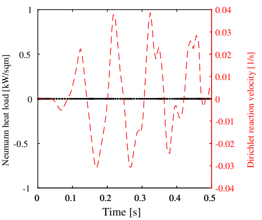

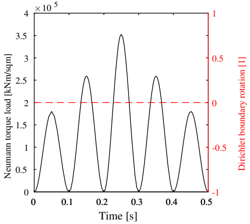

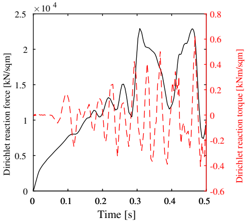

Dynamic bending/torsion of a long curved pipe (Energy-momentum error; 121-em with H8-mixed-Bbar-drill)

Errors of energy and momentum balance laws versus time (TOL = 1 J)

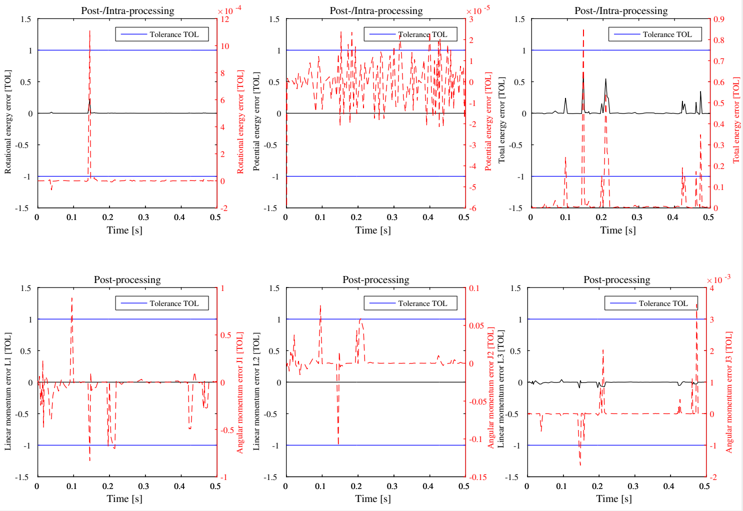

Dynamic bending/torsion of a long curved pipe
(Mesh convergence results; 121-em with H8-mixed-Bbar-drill)

Displacement of right pipe end ($T = [0, 0.5]$ s)

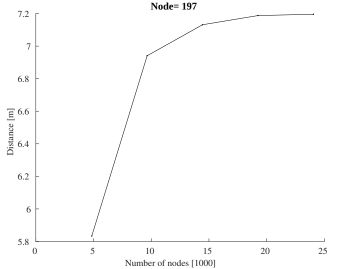

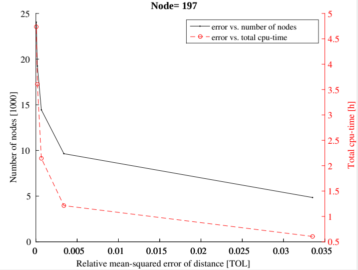

Rotation of right pipe end ($T = [0, 0.5]$ s)

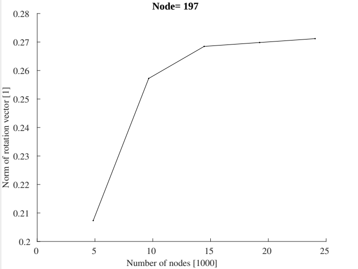

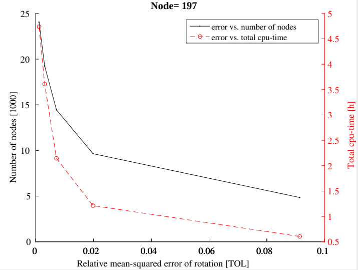

Driven rotation of a heated pipe under pressure

(Initial-boundary conditions; 121-em with H20-mixed-Bbar-drill)

Boundary Status Monitor

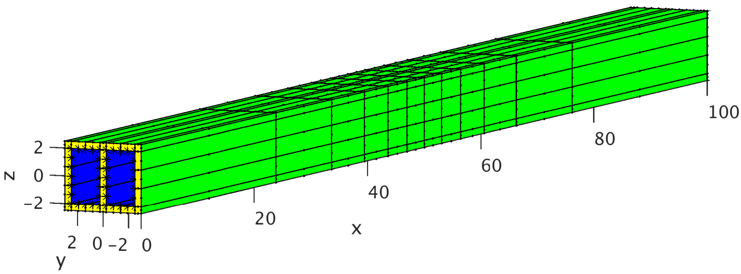

Dirichlet and Neumann boundary conditions

Yellow patches $x = 0$: Temp. $\Theta^A = \hat{\Theta}\, f(t)$, Torque $\boldsymbol{W}^A = +\hat{\boldsymbol{W}}_{\text{dri}}\, f(t)$

Yellow patches $x = 100$: Temp. $\Theta^A = \hat{\Theta}\, f(t)$, Torque $\boldsymbol{W}^A = -\hat{\boldsymbol{W}}_{\text{fri}}\, f(t)$

Blue patches: 1) Outward heat flux (cooling) with $\bar{Q}^A(t) = \hat{Q}\, f(t)$

2) Pressure follower load $p^A(t) = \hat{p}\,|\sin(\omega_{\text{load,p}}\, t)|$

Green patches: no b.c. (thermal insulation $\bar{Q}^A := 0$)

Initial conditions

$\boldsymbol{\varphi}_0^A = \boldsymbol{X}^A \quad \boldsymbol{\alpha}_0^A = \boldsymbol{0} \quad \Theta_0^A = \Theta_\infty \quad \boldsymbol{v}_0^A = \boldsymbol{0} \quad \boldsymbol{\omega}_0^A = \boldsymbol{0} \quad \Theta_\infty = 298.15$

Material Status Monitor

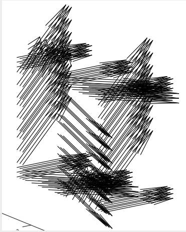

Driven rotation of a heated pipe under pressure
(Motion and loads; 121-em with H20-mixed-Bbar-drill)

Current configuration with inelastic fiber strain at $t_n = 2.0\,\mathrm{s}$

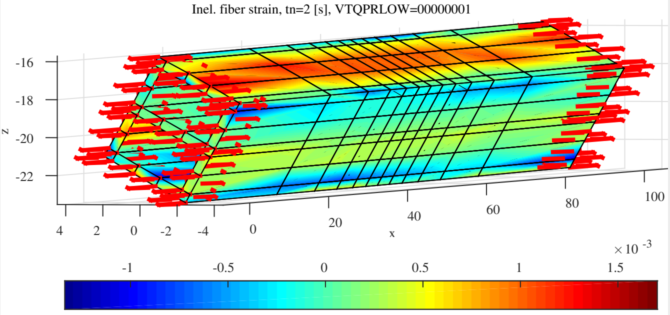

Time evolution of the loads

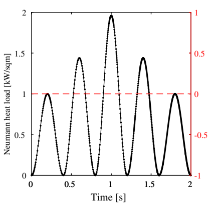

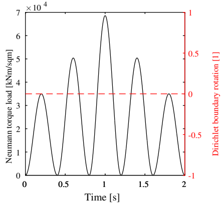

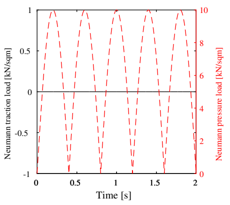

Driven rotation of a heated pipe under pressure
(Comparison of fiber viscosity; 121-em with H20-mixed-Bbar-drill)

Inelastic fiber strain in $T = [0, 2.0]\,\mathrm{s}$ (Recall viscously damped oscillations)

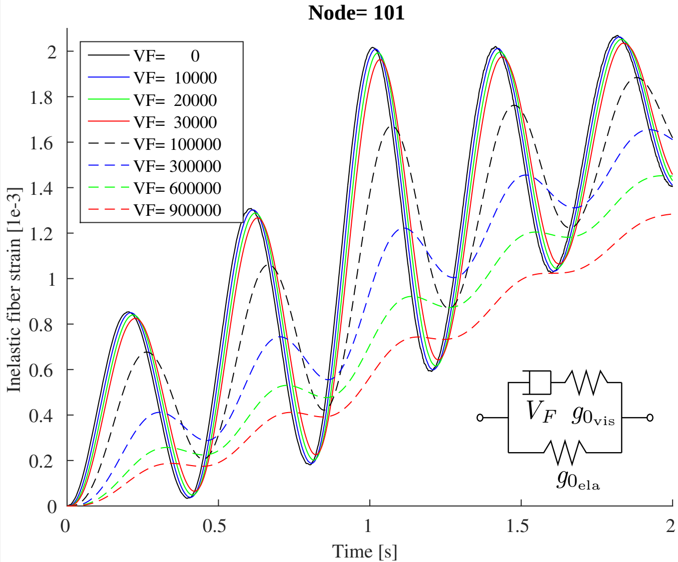

Tension bar: Displacement controlled tensile test

(Initial-boundary conditions; 121-em with H20-mixed-Bbar-drill)

Boundary Status Monitor

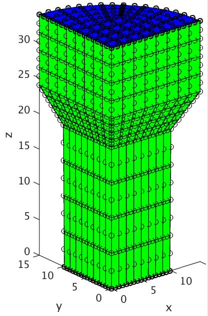

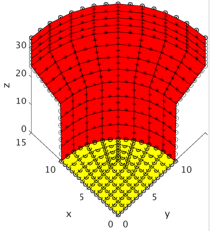

Material Status Monitor

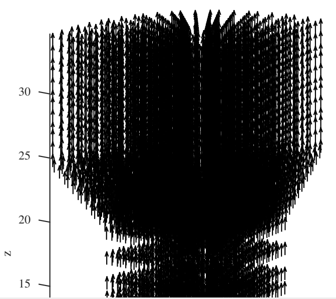

Dirichlet and Neumann boundary conditions

Blue patches: Temp. $\Theta^A = \Theta_\infty$, x^A,y^A-dofs fixed, $u_z^A = \ \ 0.1\, f(t)$

Yellow patches: Temp. $\Theta^A = \Theta_\infty$, x^A,y^A-dofs fixed, $u_z^A = -0.1\, f(t)$

Green patches: 1) y-z face $\rightsquigarrow$ x-dofs fixed, 2) x-z face $\rightsquigarrow$ y-dofs fixed

Green/Red patches: thermal insulation $\bar{Q}^A := 0$

Initial conditions

$$\boldsymbol{\varphi}_0^A = \boldsymbol{X}^A \quad \boldsymbol{\alpha}_0^A = \mathbf{0} \quad \Theta_0^A = \Theta_\infty \quad \boldsymbol{v}_0^A = \mathbf{0} \quad \boldsymbol{\omega}_0^A = \mathbf{0} \quad \Theta_\infty = 298.15$$

Tension bar: Displacement controlled tensile test (Motion and loads; 121-em with H20-mixed-Bbar-drill)

Total fiber stress at $t_n = 0.75\,\mathrm{s}$

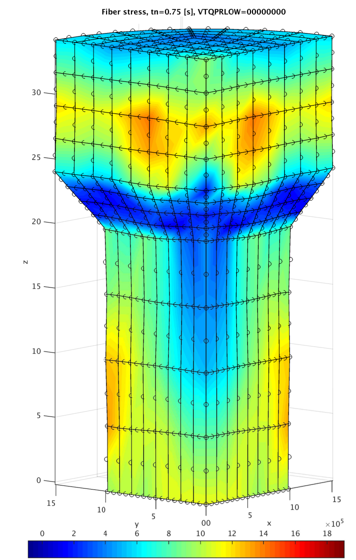

Time evolution of loads/reactions

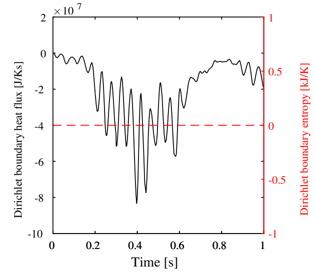

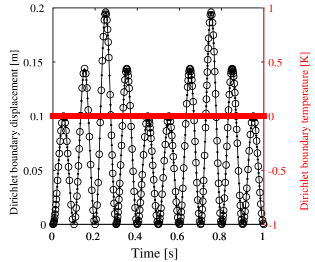

Tension bar: Displacement controlled tensile test
(Comparison of fiber stiffness; 121-em with H20-mixed-Bbar-drill)

Inelastic fiber strain at bottom (Recall driven damped oscillations)

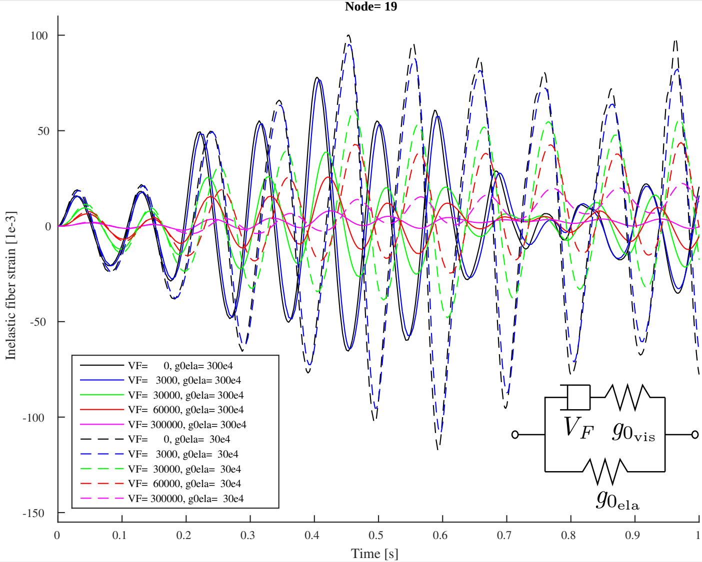

Tension bar: Displacement controlled tensile test (Mesh convergence results; 121-em with H20-mixed-Bbar-drill)

Rel. mean-squared errors in $T = [0,1]\,\mathrm{s}$: Middle part, total linear momentum

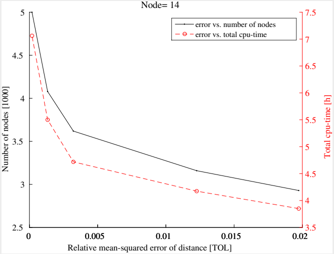

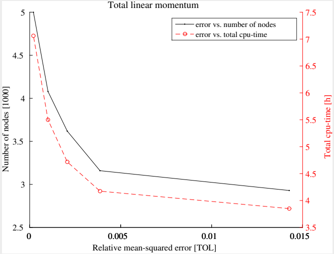

Relative mean-squared errors in $T = [0,1]\,\mathrm{s}$: Total entropy, total energy

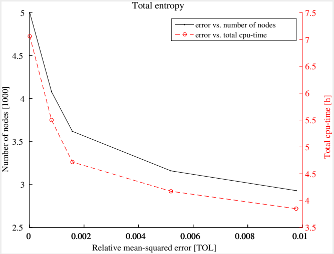

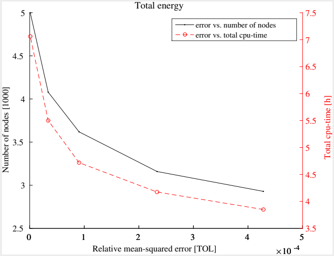

Dynamic impact test with Taylor's bar
(Initial-boundary conditions; 121-em with H20-mixed-Bbar-drill)

Boundary Status Monitor

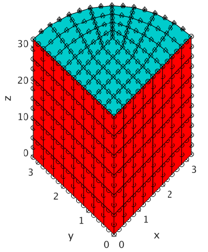

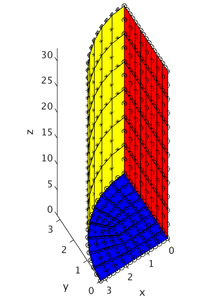

Material Status Monitor

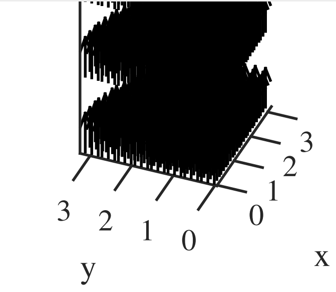

Dirichlet and Neumann boundary conditions

Red, cyan patches: thermal insulation $\bar{Q}^A := 0$ (no thermal b.c.)

Yellow, blue patches: Temp. $\Theta^A = \Theta_\infty$

Red patches: 1) y-z face $\rightsquigarrow$ x-dofs fixed 2) x-z face $\rightsquigarrow$ y-dofs fixed

Blue patches: x-y face $\rightsquigarrow$ z-dofs fixed

Initial conditions ($\Theta_\infty = 298.15$)

$$\boldsymbol{\varphi}_0^A = \boldsymbol{X}^A \quad \boldsymbol{\alpha}_0^A = \mathbf{0} \quad \Theta_0^A = \Theta_\infty \quad \boldsymbol{v}_0^A = -8\,\boldsymbol{e}_z \quad \boldsymbol{\omega}_0^A = \mathbf{0}$$

Dynamic impact test with Taylor's bar

(Motion and energies/momenta; 121-em with H20-mixed-Bbar-drill)

Current temperature at $t_n = 2.0\,\mathrm{s}$

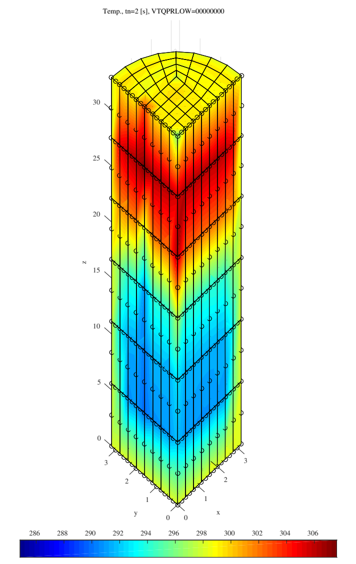

Time evolution of energies/momenta

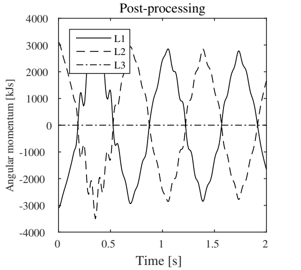

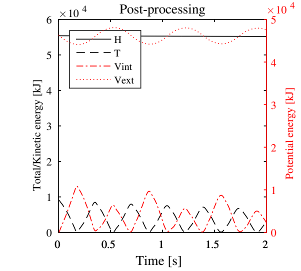

Dynamic impact test with Taylor's bar
(Comparison of fiber stiffness; 121-em with H20-mixed-Bbar-drill)

Inelastic fiber strain at bottom

(Recall defintion of the damping factor)

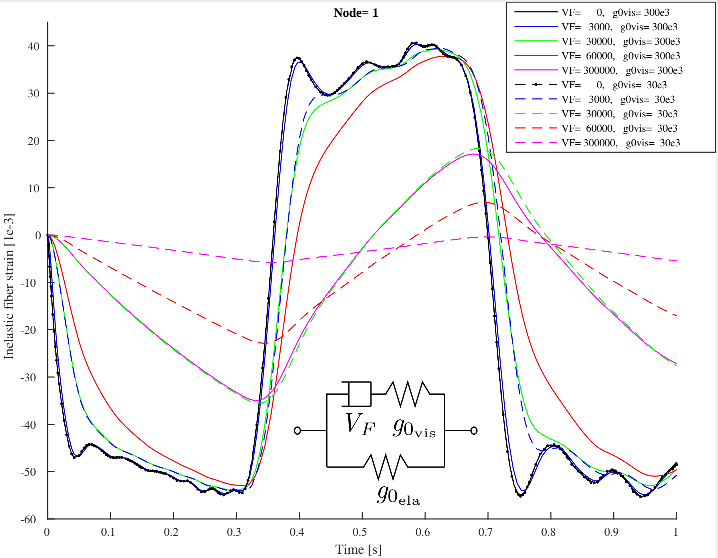

Dynamic impact test with Taylor's bar
(Mesh convergence results; 121-em with H20-mixed-Bbar-drill)

TECHNISCHE UNIVERSITÄT
CHEMNITZ

Inelastic fiber strain at bottom: Time evolutions and rela. error

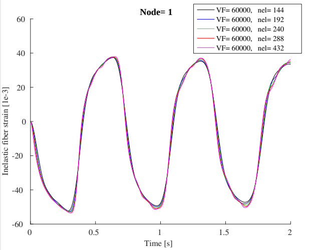

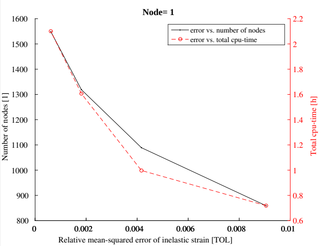

Total linear momentum: Time evolutions and relative error

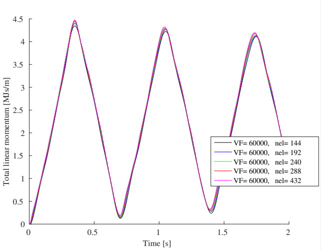

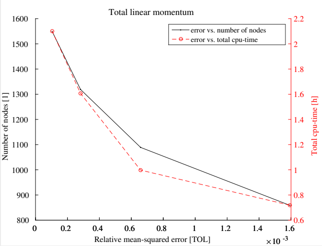

Summary

1. Motivation:
   - Dynamical FE simulations for hybrid woven composites with
   - damping and secondary effects (bending/inertia) in fabrics
2. Goals:
   - Energy-momentum schemes for generalized continua
   - derived by a variational principle with rotational DoF's
3. Strategy:
   - Variational-based two-phase thermo-viscoelasticity model with
   - mixed fields for rotation vectors and skew-symmetric stress
4. Current results:
   - Finite damping behaviour in fiber direction can be simulated by
   - hexahedrons with rotational DoF's and well mesh convergence
   - This new two-phase damping model generalizes linear effects
5. Next step:
   - Introduction of free energy functions with secondary effects

Viscously damped oscillation

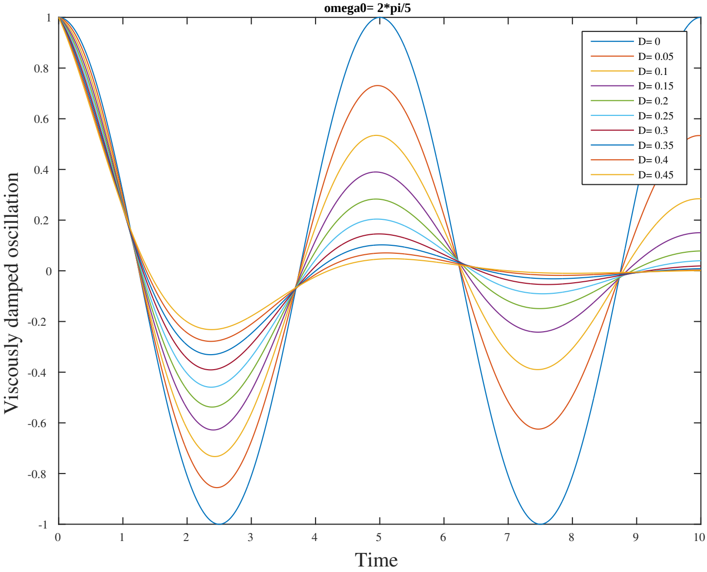

Driven viscously damped oscillation